The Coronal Mass Ejection interaction with the Induced Magnetosphere of Mars due to the 27 January 2012 Solar Storm

Authors: R. Frahm, J. R. Sharber, J. D. Winningham, H. A. Elliott Southwest Research Institute®, 6220 Culebra Road, P.O. 28510, San Antonio, Texas 78228-0510, USA
T. A. Howard, C. E. DeForest, Southwest Research Institute®,1050 Walnut, Suite 300, Boulder, CO, 80302, USA
D. Odstrêil, NASA, Goddard Flight Center, Mail Code 674, Greenbelt, MD 20771, USA
E. Kallio, Finnish Metorological Institute, Box 503, FIN-00101, Helsinki, Finland
S. McKenna-Lawler, Space Technology Ireland, Maynooth, Co. Kildare, Ireland
S. Barabash, Swedish Institute of Space Physics, Box 812,S-98 128, Kiruna, Sweden

ABSTRACT

On January 27, 2012, an X-class flare brightened on the Sun at 1815 UT. The flare generated a high-energy particle stream flowing along the Interplanetary Magnetic Field (IMF) which arrived at Mars in about 39 minutes with a Coronal Mass Ejection (CME) released from the same active region arriving at Mars several days later. The Electron Spectrometer (ELS), part of the Analyzer of Space Plasmas and Energetic Atoms (ASPERA-3) experiment on the European Mars Express (MEx) Spacecraft, is used to show that the CME plasma caused an increase in the intensity of the energy flux within the Martian magnetosheath. Models of this event predicted the speed of the CME, which is used to identify which increase of the magnetosheath signature is due to the CME, as several increases in Martian magnetosheath plasma are observed during the flare period. The Mars reaction, being an induced magnetosphere, responds to changes in solar wind conditions by continually self adjusting its magnetosheath to stand off the solar wind. Since the ion component of the solar wind interaction carries momentum away from the Sun, it is the electrons which must self adjust in order to maintain charge neutrality within the plasma and the proper induced current flow in order to stand-off changes in the solar wind.

INTRODUCTION

During February and March of 2012, the Earth and Mars were approximately radially aligned with the Sun, while in April and May they exhibited IMF alignment along the Parker spiral direction. In anticipation of this alignment, spacecraft at the Earth, Mars, and in interplanetary space individually monitored the Sun, IMF, and solar wind as well as contemporary planetary responses. Spacecraft at Venus and Mercury were also included in this monitoring program through determining off-axis effects. It is important to include the observed effects of solar wind propagation during solar storms in models of the propagation of the solar wind in the heliosphere in order to (a) improve the dynamics of solar wind propagation models and the predictability of solar wind events at other planets and (b) take into account planetary responses to solar wind drivers. To prepare for these studies, several investigative techniques were developed to determine the interaction of Mars with the solar wind and these techniques are tested here using the flare event which occurred on January 27, 2012.

In this paper we examine the interaction of Mars with the associated coronal mass ejection (CME) which occurred at the same time and from the same active region as the flare. The commencement of the in situ high-energy Solar Energetic Particle (SEP) event, X-ray, and ultraviolet light (UV) effects are discussed in a companion poster [Frahm et al., 2012].

INSTRUMENTATION

The solar wind-Mars interaction is monitored by the Analyzer of Space Plasma and Energetic Atoms (ASPERA-3) experiment on the ESA Mars Express (MEx) spacecraft. ASPERA-3 consists of an Electron Spectrometer (ELS), an Ion Mass Analyzer (IMA), and two energetic neutral atom instruments: the Neutral Particle Imager (NPI) and the Neutral Particle Detector (NPD) [Barabash et al., 2004; 2006]. ELS is a spherical top hat electrostatic analyzer (ESA) which measures electrons in the energy range 0.5 eV to 20 keV logarithmically, with a field-of-view of 4° x 360° composed of 16 azimuthal sectors, each covering 22.5° in azimuth. ELS takes 4 s to measure 127 energy samples. IMA measures ions below 40 amu from energies below 50 eV/q linearly and from 50 eV/q to 40 keV/q logarithmically, using (1) an elevation analyzer for measuring ±45° out-of-plane fluxes in 16 polar angles, approximately 5.6° wide above 50 eV/q, (2) an ESA with 96 energies over an azimuth of 360° divided into 16 sectors, each 22.5° wide and (3) an orange section style magnetic momentum analyzer dispersing into a 32 radial (mass) array along its anode.

SOLAR INITIATION

At about 1815:30 UT on 27 January 2012, the EUVI instrument on STEREO-A detected an X-class flare erupting from the active region near sunspot 1402 and at the same time, from the same active region, a coronal mass ejection (CME) was generated. About 39 minutes after the flare was observed, MeV Solar Energetic Particles (SEP) traveling along the IMF were observed at Mars. The effect of the SEP was observed to decrease to near background levels by the time the CME reached Mars and is discussed in a companion poster [Frahm et al., 2012]. In this situation, the Earth was trailing Mars and STEREO-A is located approximately 108° from the Earth-Sun line. This geometry is shown in Figure 1.

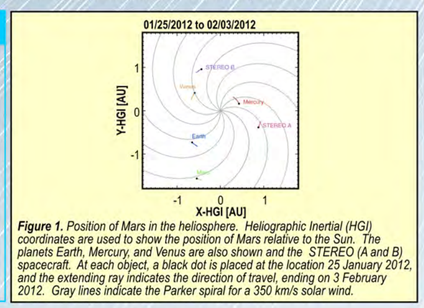

Figure 1. Position of Mars in the heliosphere. Heliographic Inertial (HGI) coordinates are used to show the position of Mars relative to the Sun. The planets Earth, Mercury, and Venus are also shown and the STEREO (A and B) spacecraft. At each object, a black dot is placed at the location 25 January 2012, and the extending ray indicates the direction of travel, ending on 3 February 2012. Gray lines indicate the Parker spiral for a 350 km/s solar wind.

CME SIMULATION

The CME was monitored and simulated using the ENLIL model of propagation in the inner heliosphere [Falkenberg *et al.,* 2011] . Figure 2 shows the CME just before the predicted encounter with Mars. The solar wind speeds show an increase at the front of the CME, encountering Mars at the CME flank. In general, the sharp speed transition indicates a shock at the CME front. Examining the model results, there appears to be velocity structure within the CME feature which has developed by the time the CME structure encounters Mars. In this paper, we examine only the response of Mars to the CME shock front.

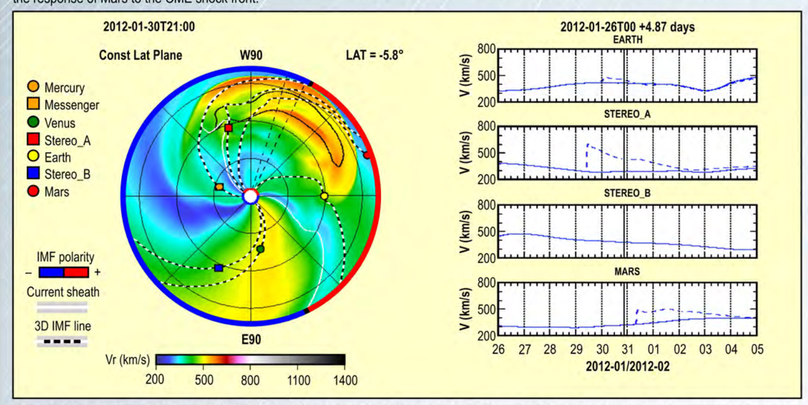

Figure 2. ENLIL model of the January 27 CME in the inner heliosphere, just before contact with Mars. The left circle contains the radial component of the solar wind speed in heliocentric Earth ecliptic coordinates, with velocities shown using the color bar at the bottom. Radial marks are every 0.5 AU and azimuthal marks are every 45°. Around the inner and outer plot boundaries is shown the IMF polarity where specific IMF field lines are shown with black and white dashed lines. Positions of the planets and monitoring spacecraft are indicated using the key at the left. The graphs at the right indicate the predicted solar wind speeds at the Earth, Mars, and STEREO A and B.

BEFORE CME ENCOUNTER

Before arrival of the CME, the magnetosphere of Mars is back to almost its steady-state response from having been disturbed days earlier by the SEP (Figure 3). In the figure the spacecraft begins (ends) in the solar wind and encounters the bow shock around Mars at about 0524 UT (0706 UT). Between 0609 UT and 0650 UT, the spacecraft is in the ionosphere around Mars and low-energy ion plasma is observed. The solar wind core is roughly below 50 eV and the halo is above 50 eV. The solar wind core electron distribution shows just above the level of spacecraft charging (Figure 4). Upon encountering the bow shock, the plasma is accelerated (Figure 5). Here the bulk of the solar wind core has been accelerated by the encounter with Mars above the level of spacecraft charging influence and a clear acceleration peak of the core electron distribution is observed. Both in-bound and out-bound encounters with the solar wind show about the same intensity of the electron distribution. Reflected in the magnetosheath, the accelerated plasma from in-bound and out-bound measurements are similar.

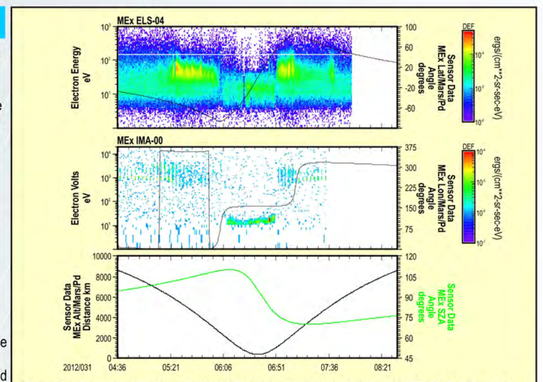

Figure 3. Mars before the arrival of the CME which was generated on January 27, 2012. Shown are the electron and ion measurements from the ASPERA-3 encounter with Mars. An ELS energy-time spectrogram of differential energy flux from sector 4 is shown at the top with the planetodetic latitude overlaid against the right axis. An IMA energy-time spectrogram of differential energy flux from sector 0 is shown in the center with the planetodetic longitude overlaid against the right axis. At the bottom is shown the spacecraft altitude (left) and solar zenith angle (right). This data from Mars is displayed with respect to the pericenter of the orbit.

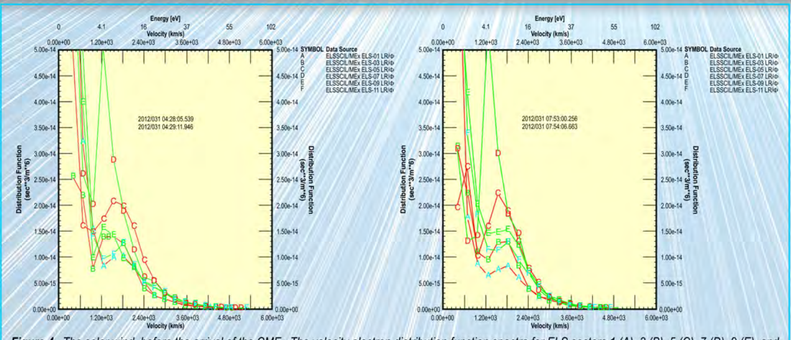

Figure 4. The solar wind before the arrival of the CME. The velocity electron distribution function spectra for ELS sectors 1 (A), 3 (B), 5 (C), 7 (D), 9 (E), and 11 (F) are shown in the solar wind both before bow shock encounter (left) and after bow shock encounter (right). Red lines mark sectors 1, 3, and 5 while green lines mark sectors 7, 9, and 11. These spectra are not corrected for spacecraft charge (about 1200 km/s) and are averaged over a 1-minute interval as far from the planet as possible.

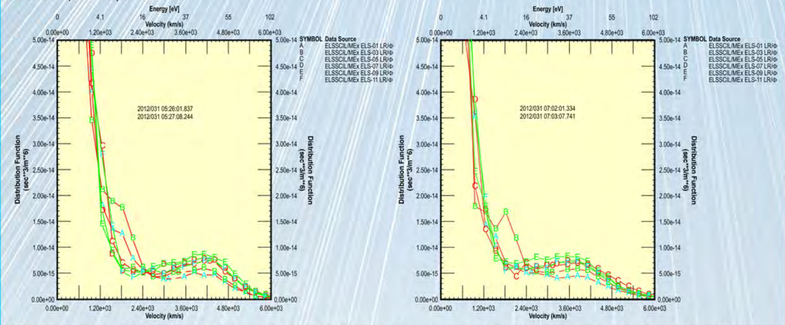

Figure 5. Mars magnetosheath spectra before arrival of the CME. These spectra are presented using the same format as those shown in Figure 4; however, they are measured in the Martian magnetosheath just inside the bow shock both before (left) and after (right) encounter with Mars; i.e., before and after the spacecraft passes through pericenter. These spectra are not correct for spacecraft charge (about 1200 km/s).- and averaged over 1 minute.

DURING CME ENCOUNTER

As the CME encounters Mars, the outer boundaries are influenced first. As can be seen in Figure 6, the solar wind before planet encounter measures a lower energy flux than after encounter. In this case, the flux intensities represented in the magnetosheath have also increased, reflecting the change in the solar wind. This situation is supported by the spectra. In Figure 7, the solar wind before encounter is similar to the previous case (Figure 4) before the encounter, but the core is accelerated and the core density has increased after encounter. These solar wind distributions are taken as far from the bow shock as possible, but Figure 6 suggests that just before the in-bound bow shock is encountered (1224 UT) the solar wind intensity increases. The magnetosheath distributions (Figure 8) show that indeed they are responding to changes in the solar wind. The in-bound magnetosheath spectra show increased density and acceleration compared to the values before the CME is encountered, and the solar wind must continue to increase for the out-bound magnetosheath response to show even greater density and acceleration. In addition, there is more separation in the spectra measured by the different sectors of ELS suggesting an asymmetric flow. Thus, as the ions respond to changing flow conditions associated with the CME impact, the electrons are adjusting by changing their flow along the magnetic field in order to balance charge separation.

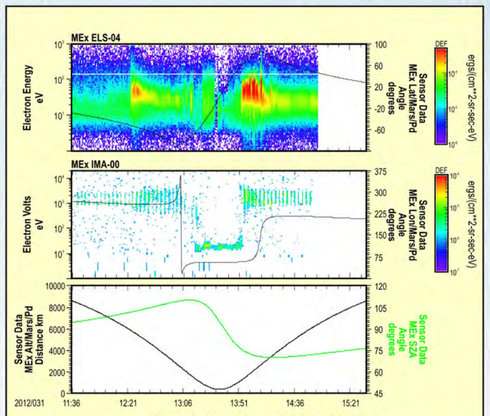

Figure 6. Mars during arrival of the CME.

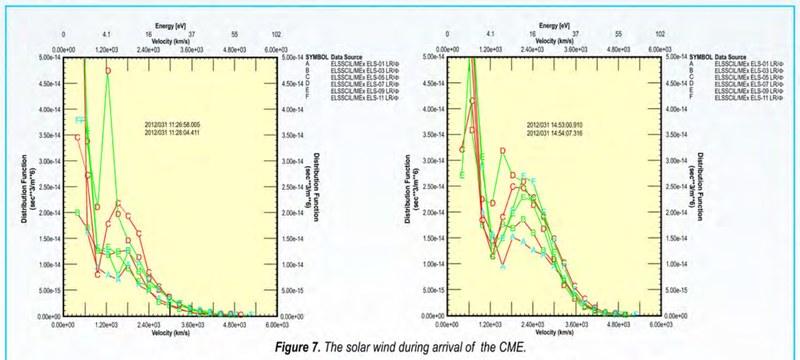

Figure 7. The solar wind during arrival of the CME.

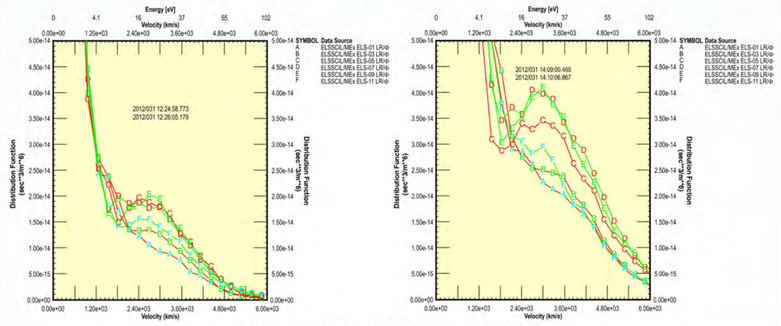

Figure 8. Mars magnetosheath spectra during arrival of the CME.

AFTER CME ENCOUNTER

The overview after the initial CME shock passage is indicated in Figure 9. Here we see that the in-bound and out-bound magnetosheaths sampled by the pass exhibit an increase in energy flux, but the altitude of the bowshock measurements is roughly the same through out the encounter. The energy deposited by the CME has propagated down to the ionosphere on the day side and ionosphere heating is occurring as the flux of the low-energy ions has increased.

As the initial CME shock front passes Mars, the solar wind spectra (Figure 10) show that the density decreases, but the amount of acceleration is higher than before the encounter. The magnetosheath response (Figure 11) indicates that the density in the outbound sheath is lower than that of the inbound sheath, although they are accelerated to about the same level. In addition In could be that multiple regions of the CME having different physical characteristics are being encountered. Examination of the CME simulation shows multiple shocks encounter Mars and the CME structure is made up of multiple crossings of shocks within the CME (Figure 2).

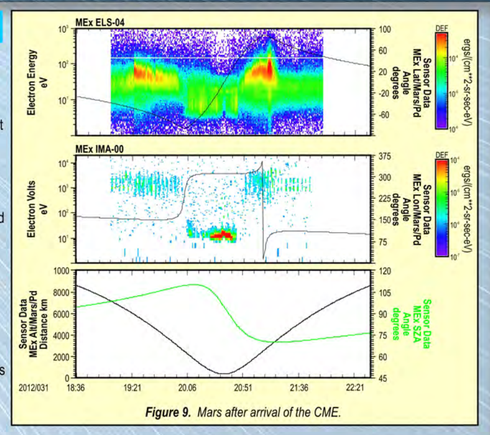

Figure 9. Mars after arrival of the CME.

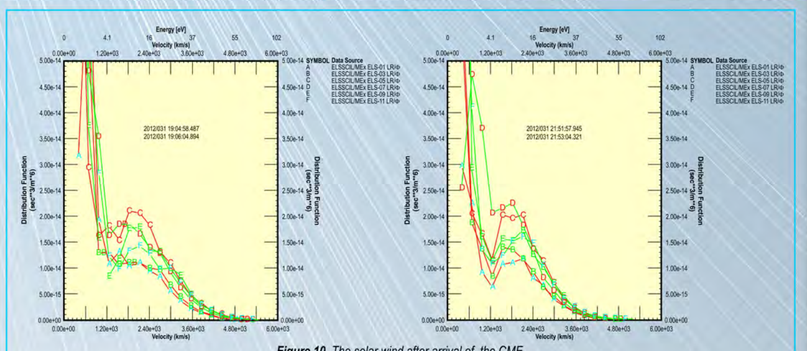

Figure 10. The solar wind after arrival of the CME.

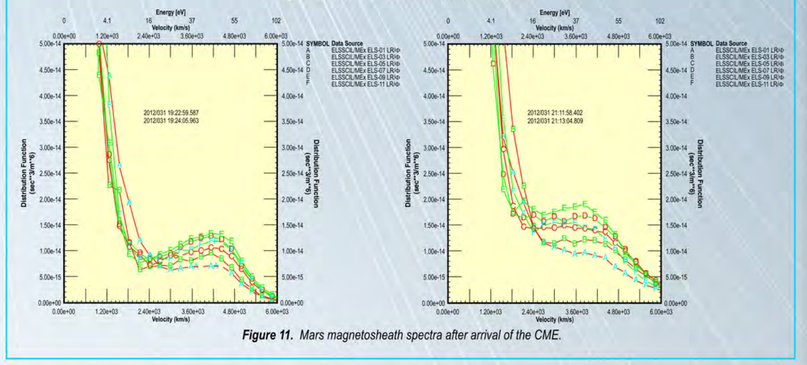

Figure 11. Mars magnetosheath spectra after arrival of the CME.

Future investigation of this CME will include a more detailed analysis of the solar wind. The core-halo description of the solar wind characteristics can be generated at a shorter time resolution than shown here. These characteristics can be generated through the magnetosheath because this plasma, shocked by the planet, is accelerated solar wind plasma. Comparisons before, during, and after should reveal more details about the solar wind structure of the CME. Acceleration and heating of the distributions in the magnetosheath are the response of the planet and should also be revealed. This will require an identification and separation of the effects of the solar wind driver and the planetary response.

CONCLUSION

A CME was launched from the Sun on January 27, 2012. The initial CME shock encountered Mars on January 31 sometime between about 1200 UT and about 1400 UT. An examination of particle spectra obtained during three MEx passes encompassing the CME arrival at MARS was made to study the effect of the CME on particle energy and density. During the CME encounter energy is transferred to the magnetosheath around Mars, eventually propagating down to transfer energy to the ions in the ionosphere. Simulations suggest that this CME exhibited multiple shock behavior. This effect was not studied in this investigation; however, spectral characteristics of the last magnetosheath encounter (shown in Figure 11) suggest that multiple CME fronts may have encountered the Mars system. Further study is required to investigate this question.

REFERENCES

Barabash, S., *et al.,* , ASPERA-3: Analyser of space plasmas and energetic atoms for *Mars Express, In Mars Express – The Scientific Payload,* ESA SP-1240, 121-139, 2004.

Barabash, S., *et al.,* The analyzer of space plasmas and energetic atoms (ASPERA-3) for the Mars Express mission, *Space Sci. Rev., 126 (1-4),* 113-164, DOI: 10.1007/s11214-006-9124-8, 2006.

Falkenberg, T. V., *et al.,* Evaluating predictions of ICME arrival at Earth and Mars, *Space Weather, 9(9),* S06002, doi:10.1029/2010SW000642, 2011.

Frahm, R. A. J. R. Sharber, J. D. Winningham, H. A. Elliott, T. A. Howard, C. E. DeForest, D. Odstrčil, E. Kallio, S. McKenna-Lawler, and S. Barabnash, Solar Energetic Particle Arrival at Mars due to the 27 January 2012 Solar Storm, poster presented at Solar Wind 13, Kona, Hawaii, June 2012.

ACKNOWLEDGEMENTS

This investigation involving the ASPERA-3 data are supported at Southwest Research Institute under NASA contract NASW-00003, at the Swedish Institute of Space Physics by the Swedish National Space Board, and through ESA, the first European mission to the red planet. Investigation with the STEREO data was supported at Southwest Research Institute. The SECCHI data are produced by a consortium of international groups, including NASA/GSFC (US), RAL (UK), NRL (US), UBHAM (UK), MPS (Germany), CSL (Belgium), and IOTA and IAS (France). TAH is supported in part by the NSF SHINE competition (ATM-0849916) and both TAH and CED are supported in part by NASA Grant NNX10AC05G. Thanks to C. A. Gonzalez, S. J. Jeffers, J. K. Jennings, R. O. Menchaca, J. Mukherjee, and M. A. Muller.

Po0629